Identification of Gait Events using Expert Knowledge and Continuous Wavelet Transform Analysis

Siddhartha Khandelwal and Nicholas Wickström
Intelligent Systems Laboratory, Halmstad University, Box 823, SE-301 18, Halmstad, Sweden

Keywords: Gait Event Detection, Wavelet Analysis, Accelerometers, Outdoor Walking, Continuous Wavelet Transform.

Abstract: Many gait analysis applications involve long-term or continuous monitoring which require gait measurements to be taken outdoors. Wearable inertial sensors like accelerometers have become popular for such applications as they are miniature, low-powered and inexpensive but with the drawback that they are prone to noise and require robust algorithms for precise identification of gait events. However, most gait event detection algorithms have been developed by simulating physical world environments inside controlled laboratories. In this paper, we propose a novel algorithm that robustly and efficiently identifies gait events from accelerometer signals collected during both, indoor and outdoor walking of healthy subjects. The proposed method makes adept use of prior knowledge of walking gait characteristics, referred to as expert knowledge, in conjunction with continuous wavelet transform analysis to detect gait events of heel strike and toe off. It was observed that in comparison to indoor, the outdoor walking acceleration signals were of poorer quality and highly corrupted with noise. The proposed algorithm presents an automated way to effectively analyze such noisy signals in order to identify gait events.

1 INTRODUCTION

Gait is generally defined as the manner or way of walking. The healthy locomotor system integrates input from the motor cortex, cerebellum, and the basal ganglia, as well as feedback from visual, vestibular and proprioceptive sensors to produce controlled motor commands that result in coordinated muscle firings and limb movements (Hausdorff, 2007). This multi-level neural-locomotor control system produces a stable gait and a highly consistent walking pattern while improper co-ordination may lead to deviations from normal gait behavior resulting in unstable gait. Gait analysis involves measuring and understanding various parameters of gait to interpret and draw conclusions on physiological, pathological and psychological factors modulating healthy or unhealthy gait. In recent years, technological advances have made it possible to develop better techniques for gait analysis and as such its applications have grown manifold. It can be used to design and optimize functional electrical stimulation (FES) systems (Williamson and Andrews, 2000; Mansfield and Lyons, 2003), clinical tool for diagnosis and severity analysis of neurophysiological disorders and impairments (Socie et al., 2013), elucidate the working of our neuro-locomotory system (Hausdorff, 2007), assess the quality of gait of amputees and rehabilitating patients (Aminian et al., 2004; Selles et al., 2005), recognize different walking behaviors (Hafner and Bachmann, 2008), predict and evaluate the risk of falls in older adults (Reelick et al., 2009; Callisaya et al., 2010) and many more.

Gait is comprised of sequential gait cycles and each such gait cycle is composed of a sequence of events that mark the transition from one gait phase to another (Rueterbories et al., 2010). In the temporal domain, gait events are expressed as a function of time while in the spatial domain, gait movements are expressed as a function of the orientation of the limbs and joints. In terms of temporal domain parameters, the two most relevant events in a normal gait cycle are the initial heel contact or heel strike (HS) and terminal contact or toe off (TO). Both these key events are widely used in gait analysis because of the aforementioned applications and the fact that other temporal parameters like swing, stance and stride time can be directly computed from them. Thus detecting HS and TO accurately is of vital importance in clinical gait analysis and many sensors have been used to this end.

Force plates and camera-based motion capture (mocap) systems are considered as the "gold standard" or reference for identifying gait events (Miller,

Khandelwal S. and Wickström N..
Identification of Gait Events using Expert Knowledge and Continuous Wavelet Transform Analysis.
DOI: 10.5220/0004799801970204
In *Proceedings of the International Conference on Bio-inspired Systems and Signal Processing* (BIOSIGNALS-2014), pages 197-204
ISBN: 978-989-758-011-6

2009; Desailly et al., 2009). Force plates capture the ground reaction force caused by the pressure exerted by the foot on them. Thus by applying simple thresholds on the recorded force, individual events of HS and TO can be precisely identified (Mills et al., 2007). Camera-based mocap systems track markers that are placed on the body (Hanlon and Anderson, 2009; Aung et al., 2013). Generally, a laboratory setup consists of a pair of force plates (one for each foot) that is used concurrently with the mocap system. Though these devices provide relatively precise measurements, they are highly expensive, immobile and require competence in maintenance, operation and execution. The fact that they record the information of only a couple of steps renders them inadequate for applications that need long-term or continuous gait monitoring. For example, some authors have hypothesized that in-coordination between the neural and locomotor control systems results in specific gait patterns which can be used for analyzing neurophysiological disorder patients (Stolze et al., 2004; Hausdorff, 2007) or older adults that have a fear of falling (Herman et al., 2005; Reelick et al., 2009). These applications would essentially require mobile sensors and robust gait analysis algorithms for day-to-day monitoring of such patients.

Pressure sensitive mats and foot switches provide the option of being used outside the laboratory for measuring gait events. The pressure sensitive mat (e.g.GaitRite) consists of a grid of pressure sensors that can be few meters in length (McDonough et al., 2001). Foot switches like force sensitive resistors can be attached at various positions below the feet or insoles of the shoe (Williamson and Andrews, 2000; Aminian et al., 2002; Lau and Tong, 2008). However there have been studies to show that they are less reliable and not durable over longer periods (Mansfield and Lyons, 2003) and cannot differentiate between foot load changes due to walking and those caused by weight shifting for non-walking tasks (Pappas et al., 2001). Hence, from a long-term perspective, they might not be convenient for outdoor use in daily life and be prone to mechanical failures. Moreover, these sensors provide only temporal information and thus restrict the scope for any further analysis involving spatial parameters of gait.

Consequently, for such long-term gait monitoring and daily life applications, an alternative is to use wearable inertial sensors like accelerometers and gyroscopes. Advancements in MEMS technology have made them miniature, low-powered, durable, inexpensive, highly mobile and readily available (Kavanagh and Menz, 2008). In recent years, many gait event identification algorithms have been developed using inertial sensors (Rueterbories et al., 2010). While some have used gyroscopes (Pappas et al., 2001; Aminian et al., 2002; Lee and Park, 2011), others have found it appropriate to use accelerometers (Williamson and Andrews, 2000; Mansfield and Lyons, 2003; Selles et al., 2005; Hanlon and Anderson, 2009; Sant'Anna and Wickström, 2010; Aung et al., 2013). A major drawback of using inertial sensors is that they provide highly noisy information and thus require very robust algorithms for gait analysis. Based on the quality and type of information they provide, some authors have discussed the pros and cons of using either accelerometers or gyroscopes (Aminian et al., 2002; Lau and Tong, 2008) though it must be noted that these sensors are used and well researched in other fields like aerospace and humanoids (Khandelwal and Chevallereau, 2013). In the context of gait event analysis, accelerometers seem to be a better choice than gyroscopes for developing automated gait event identification systems. Sudden movements like jerks or turns during walking would cause large gyro drift errors. Furthermore, gyroscopes have high power consumption, long reaction time and are very sensitive to temperature effects limiting their long-term outdoor use (Tan and Park, 2005; Woodman, 2007). Accelerometers, on the other hand, suffer from noise due to mechanical vibrations and calibration errors but these do not diverge in time and in many cases can be handled effectively.

Recently, many methods have been developed for identifying gait events only from accelerometer data. Some of these algorithms apply different techniques to analyze signals obtained from individual accelerometer axis (Williamson and Andrews, 2000; Mansfield and Lyons, 2003; Selles et al., 2005; Torrealba et al., 2010). Hence, at the beginning of the experiment, the accelerometer is positioned in some specific orientation such that each accelerometer axis is aligned with some pre-defined limb axis and the assumption is made that the accelerometer shall stay statically positioned during the entire movement of the experiment. Otherwise, either the axis alignment should be readjusted frequently or the exact orientation of the accelerometer must be known throughout the experiment (which might be difficult to estimate) to compensate for the misalignment of the axes. A possible alternative could be to analyze the resultant accelerometer signal instead as it is invariant to individual axis alignment. Some other methods use machine learning techniques (Williamson and Andrews, 2000; Aung et al., 2013) but the difficulty with such algorithms is that they depend on labeled training data and the addition or exclusion of any parameter would require re-training the entire algo-

rithm. In recent years, wavelet transforms are being increasingly used to develop gait event detection algorithms (Aminian et al., 2002; Forsman et al., 2009; Gouwanda and Senanayake, 2009; Aung et al., 2013) as it supports simultaneous time frequency analysis of non-stationary signals and have been shown to be robust among peak detection algorithms (Yang et al., 2009). Additionally, baseline trends can be implicitly removed and no preprocessing of the signal is required (Du et al., 2006). All methods and techniques that were reviewed in this paper have been developed by 'simulating a physical world environment inside a controlled laboratory'. Therefore there is a need for a robust algorithm that can identify gait events from acceleration signals collected in the 'outdoor environment'.

This paper proposes a novel algorithm for the robust identification of gait events from accelerometer data collected during indoor and outdoor walking. The developed method combines the knowledge about some known gait characteristics referred to as expert knowledge (EK) with continuous wavelet transform (CWT) analysis of the resultant accelerometer signal. The proposed method is applied on an indoor walking dataset to evaluate its efficiency and accuracy. The robustness of the algorithm is evaluated by applying it on outdoor walking signals and comparing the mean stride time calculated from the left and right legs of each subject. Since the outdoor walking signals were of poorer quality and noisier than indoor, further analysis was required to identify the gait events. The rest of this paper is organized into four sections. Sections 2 & 3 describe the data collection procedure and the developed algorithm, respectively. Section 4 presents the results while Section 5 concludes this paper and discusses future work.

2 EXPERIMENTS

Fifteen healthy volunteers participated in the experiments with informed prior consent. Each subject had two Shimmer (3-axis) accelerometers (sampling at 128 Hz) attached to both their ankles, just above their lateral malleolus. Velcro straps were used to keep the sensors in place. The subjects were instructed to walk for about 25 minutes at their preferred walking speed on an outdoor street which was not absolutely flat and made of asphalt concrete. The proposed method was also applied on a previously published dataset which was collected from 6 subjects walking inside a laboratory (Sant'Anna and Wickström, 2010). The experiment used two Shimmer 3-axis accelerometers (sampling at 50 Hz) positioned at the ankles and a 6m long Gold GaitRite pressure sensitive mat (sampling at 60 Hz) which had its own software for detecting HS and TO. The pressure mat data was used as the ground truth. All analysis was performed in MATLAB (MathWorks, Natick, Massachusetts, USA).

3 METHODOLOGY

3.1 Continuous Wavelet Transform

The wavelet transform produces a time frequency decomposition of the signal which separates individual signal components more effectively than the short-time Fourier transform. The ability to give the time localization of the spectral components in a non-stationary signal has rendered it a powerful tool for processing of biosignals like EEG, EMG and ECG (Rafiee et al., 2011). Wavelet transforms can be mainly divided into discrete and continuous forms. The former operates over scales and positions based on powers of two making it non-redundant, computationally more efficient and sufficient for reconstruction of signal. The latter allows transforms at all scales and positions, thus maintaining all information without down-sampling which makes it appropriate for tasks like peak detection (Du et al., 2006) and pattern matching. The Continuous Wavelet Transform or CWT of a signal, $x(t)$, is given as:

$$CWT(a,b) = \frac{1}{\sqrt{a}} \int_{-\infty}^{+\infty} x(t)\psi^*(\frac{t-b}{a})dt \qquad (1)$$

where $\psi^*(t)$ is the complex conjugate of the wavelet function $\psi(t)$ and a and b are the dilation and location parameters of the wavelet, respectively (Mallat, 1999). $\psi(t)$, usually termed the mother wavelet function, must satisfy certain mathematical criteria like finite energy and no zero-frequency component to be admissible (Addison, 2005). The dilation or scale is inversely proportional to the spectral components. Low scales or high frequencies provide more local information while high scales or low frequencies provide relatively more global information about the signal. This multi-resolution property of CWT makes it appropriate for gait analysis.

3.2 Expert Knowledge

There are some characteristics that are particular to gait signals which is used in conjunction with CWT analysis to develop the proposed algorithm. These known gait characteristics, namely, $EK_{1,2,3}$ are enumerated below:

1. For a subject walking at their preferred walking speed, the shape of the HS regions in the resultant accelerometer signal have consistency throughout the signal as shown in Figure 1a. TO regions have a similar consistency but their peaks are lower than HS because normally the heel strikes the ground with higher force compared to the toe lifting off the ground.
2. The activity of walking cannot be done at arbitrarily high speeds. There is an upper bound in the frequencies that are generated during walking.
3. This is an extension of EK_2. During walking at preferred walking speed, the velocity might change with fairly consistent stride time but there is no random high jump in speed from one step to the other. For example if one step is taken at x m/s then the following next step cannot be at $1.5x$ m/s for a 'normal' walk.

Each of these facts are utilized to develop the proposed method. Figure 1a shows the resultant acceleration signal that is calculated from the individual accelerations from each axis of the 3-axis accelerometer. EK_1 is used to choose the mother wavelet that is applied to this resultant acceleration signal. The CWT gives continuous wavelet coefficients which illustrate how well a wavelet function correlates with a specific signal. Thus greater the correlation, higher will be the CWT coefficients and vice-versa. The wavelet 'symlet-4' (sym4) is chosen as the mother wavelet function $\psi(t)$ which is near symmetric and orthogonal (Figure 1b). Sym4 wavelet highly matches or correlates with the HS regions giving sharper peaks at higher scales (called ridges) more than the TO regions, thus providing a better separation between them at the same scales. EK_2 is used to choose the appropriate scales for further analysis. As shown in Figure 2, the information on lower scales corresponds to high frequency noise and artifacts which can be ex-

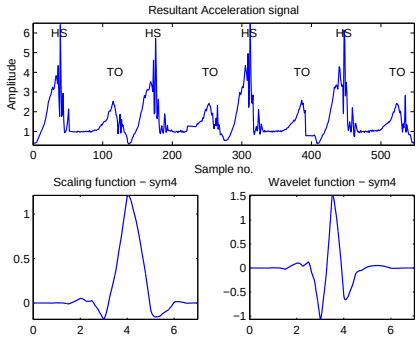

Figure 1: (a) HS and TO regions in the resultant acceleration signal from outdoor walking. (b) Scaling and wavelet functions of sym4 wavelet.

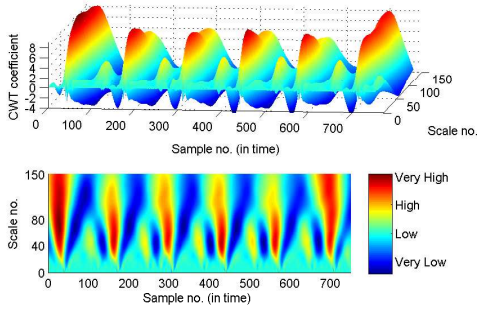

Figure 2: CWT coefficients of the resultant acc. signal.

cluded. This is one of the many advantages of CWT analysis as no pre-processing of the signal like noise filtering or smoothing is required. The scales that are chosen for further analysis are where the CWT coefficients for the matched HS region are high and form sharp ridges. In this case, as shown in Figure 2, the CWT coefficients are very high between scales 40 to 80. Thus they are chosen for further analysis and these scale bounds are applied to the resultant acceleration signals of all subjects. EK_3 is used in the statistical diagnosis of stride time to automatically detect the inconsistent HS and TO regions (explained in Section 3.3.2 and 3.3.3).

3.3 Identification of Gait Events

3.3.1 Detecting the good HS

According to Eq.1, the CWT of the acceleration signal results in a CWT coefficients matrix or *CCM* that is based on the scale and location parameters of the sym4 wavelet. Each row of this matrix corresponds to a chosen scale of the wavelet while each column corresponds to that sample of the acceleration signal where the wavelet is positioned or located. Thus an element in this matrix represents the correlation between the wavelet and a signal sample at a given scale. The *CCM* matrix has a size *mxn* where *m* is the total number of chosen scales and *n* is the total length of the vector of the samples of the acceleration signal. The maximum coefficient value in each column of the *CCM* matrix represents the best matching for that signal sample from all chosen scales. A vector MC_{1xn} is defined which contains the maximum coefficient values from all *n* columns. A rough envelope (RE) of the HS regions is obtained by subtracting the mean of *MC* from *MC* and retaining all non-negative values from the result (refer Figure 3a):

$$RE_{1xn} = \begin{cases} MC - \overline{MC} & \text{if } MC - \overline{MC} \geq 0 \\ 0 & \text{if } MC - \overline{MC} < 0 \end{cases} \quad (2)$$

where $MC = max(CCM)$ and $\overline{MC} = mean(MC)$.

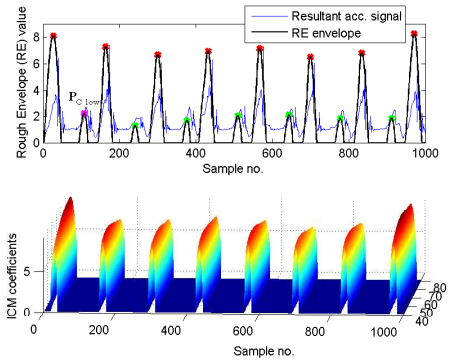

Figure 3: (a) Rough envelope (*RE*) of the HS and TO regions. Red and green dots represent peaks that belong to the C_{high} and C_{low} clusters respectively. The magenta dot represents P_{C-low}. (b) Coefficients of the *ICM* matrix.

Then all local maxima points or peaks in the rough envelope are found and separated into two clusters using k-means clustering. One cluster, C_{high}, comprises high-valued peaks located in the HS regions while the other cluster, C_{low}, comprises low-valued peaks from the TO regions (Figure 3a). The peak with the highest value in the C_{low} cluster is identified and labeled as P_{C-low}. All coefficients greater than $(P_{C-low} + \overline{MC})$ in the CWT coefficients matrix would approximately correspond to only the HS regions. Thus an intermediate coefficients matrix (ICM_{mxn}) is created from the original CWT coefficients matrix by setting all coefficients less than $(P_{C-low} + \overline{MC})$ to zero:

$$ICM = \begin{cases} CCM & \text{if } CCM > (P_{C-low} + \overline{MC}) \\ 0 & \text{if } CCM \leqslant (P_{C-low} + \overline{MC}) \end{cases} \quad (3)$$

The ICM coefficients (shown in Figure 3b) represent the probable HS event with sharp ridges. By computing the local maxima along the columns in the *ICM* matrix, the ridges that correspond to the occurrence of HS events are obtained, as shown in Figure 4. The mean of local maxima points making each ridge in the *ICM* matrix gives the **good HS** events in the resultant acceleration signal. For a good quality signal with a high signal to noise ratio (SNR), all HSs will probably be identified in this step which was the case with the indoor walking dataset. However, the acceleration signals collected during outdoor walking were highly noisy with poor SNR. For such signals, it is observed that few HS and TO regions are irregularly shaped, i.e. they look different from the regular HS and TO regions due to signal corruption, sampling effects or other factors influencing noise (some examples are shown in Figures 5 and 6). Due to their irregular and inconsistent shape, these **noisy HS** regions do not match with the sym4 wavelet as much as the other regular HS regions and lead to lower peaks that

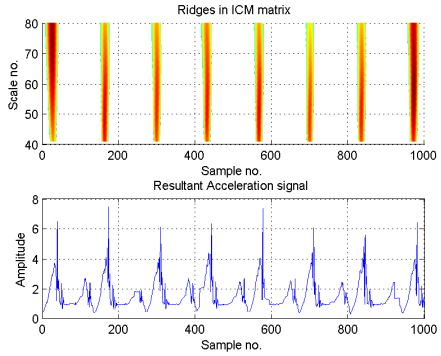

Figure 4: Ridges in the *ICM* matrix that correspond to HS.

do not fall in the C_{high} cluster. As a result, the ridges corresponding to these noisy HSs do not appear in the *ICM* matrix and are undetected in this step. Similarly it might be that the **noisy TO** regions might get incorrectly identified as HS due to high peaks that fall in the C_{high} cluster. Using EK_3, a statistical analysis of stride time allows us to automatically detect these irregular HS and TO regions and identify them correctly. Henceforth the terms 'noisy HS' and 'noisy TO' are used to represent the HSs that were undetected and TOs that were misidentified as HSs, in this step, respectively.

3.3.2 Locating the Noisy HS Events

The ridges corresponding to the noisy HS regions go undetected in the previous step. An automated way to find these missed HSs is by statistically investigating stride time. Stride time is defined as the periodic time between any two gait events such as HS. Using $EK_{2,3}$ it can be deduced that the stride time values which are greater than 1.5 times the median stride time (appear as high outliers in the boxplot of stride time in Figure 5) correspond to the noisy HSs. From each of these high outliers, the HS event before and after the missed HS event can be identified by referring to the vector of good HSs obtained in Section 3.3.1. A temporal boundary can be set to search for the missed ridges of the noisy HSs in the *CCM* matrix:

$$\begin{aligned} bound_{low} &= HS_{before} + Q1 \\ bound_{high} &= HS_{after} + Q3 \end{aligned} \quad (4)$$

where HS_{before} and HS_{after} are the HS events before and after the missed HS and $Q1$ and $Q3$ are the 1st and 3rd quartiles of stride time. The mean of the local maxima points making each of these missed ridges in the *CCM* matrix gives the location of the noisy HS events which are appended to the vector of HSs. The stride time is recomputed at the end of this step.

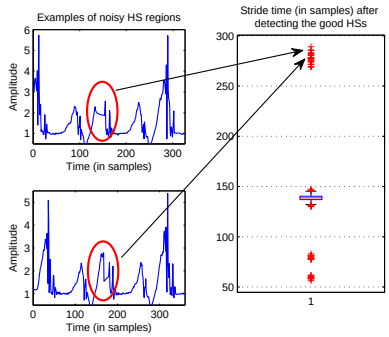

Figure 5: Examples of noisy HS regions (circled in red) that can be statistically detected from stride time.

3.3.3 Removing the Noisy TO Events

As explained in Section 3.3.1, the noisy TOs are the ones which have been misidentified as HS and can be automatically detected and removed in a similar statistical fashion as above using EK_3 and stride time. Figure 6 shows the boxplot of stride time. The noisy TOs lie in the cluster of outliers below the lower whisker of stride time. These outliers correspond to stride time values below $(Q1 - 1.5 * IQR)$ where $Q1$ is the first quartile and IQR is the interquartile range of stride time. A noisy TO always give rise to a consecutive outlier pair among these low outliers. Such a pair consists of one outlier which corresponds to the distance between the previous HS and the noisy TO and the other outlier which corresponds to the distance between this same noisy TO and the next HS. This pair of outliers would be indexed consecutively in the vector of HSs because they occur one after the other as shown in Figure 6. Thus by identifying such outlier pairs, the noisy TOs that have been misidentified as HSs are removed from the vector of detected HSs.

3.3.4 Final HS and TO Events

At the end of executing the previous three steps, the conclusive HS events are obtained in the given acceleration signal. The TOs are detected by looking for the ridges between two HSs in the *CCM* matrix that are created by matching of the wavelet with TO regions (Figure 2) .

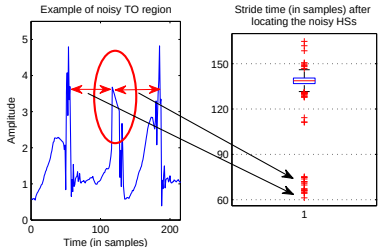

Figure 6: Example of noisy TO region (circled in red) that creates an outlier pair in the boxplot of stride time.

4 RESULTS

Section 3 presents a four step procedure to systematically identify the gait events of HS and TO:

1. Detect the good HS events: Identifies the HS from the ridges in the *ICM* matrix that correspond to the consistent and regularly shaped HS regions. Stride time is computed at the end of this step.
2. Locate the noisy HS events: Detects the missed HS events in step 1 (that correspond to the irregularly shaped noisy HS regions) by searching for the missed ridges in *CCM* matrix within the defined temporal bounds.
3. Remove TO incorrectly identified as HS: Detects and removes the irregularly shaped TO regions misidentified as HS in step 1, by identifying lower outlier pairs in stride time values that are consecutively indexed in the vector of HSs.
4. Final HS and TO events: Conclusive HS and TO events in the given acceleration signal.

Figure 4 corresponds to step 1 while Figure 7 shows the stride time at the execution of steps 2, 3 and 4; by applying the proposed method on a subject's accelerometer signal from outdoor walking. The noisy HSs and TOs are seen as long spikes which subsequently get removed after the execution of each step.

The developed algorithm was first applied on an indoor walking dataset consisting of 6 subjects. Since these signals had high SNR, steps 1 and 4 were sufficient to detect the HS and TO of all subjects. Table 1 shows the mean absolute error and standard deviation in detecting HS and TO using the proposed algorithm in comparison with the results of symbolic approach and peak detection reported in (Sant'Anna

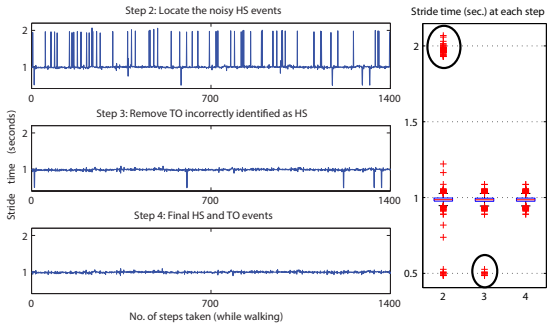

Figure 7: Stride time (seconds) at steps 2, 3 and 4 while processing an outdoor walking acceleration signal.

and Wickström, 2010), that were applied to the same dataset. The errors were calculated by comparing the detected gait events with the ground truth. In the proposed method there was a constant bias of 5 samples between the identified TO in the signal and the ground truth given by the pressure mat. This could be due to the fact that the pressure mat registers a TO when the toe leaves the mat to enter the swing phase while the proposed algorithm detects the TO when the toe presses against the ground just before the lift, during which there is highest resultant acceleration in the TO region. This constant bias has been removed while computing the mean absolute error and standard deviation of TO presented in Table 1.

The developed algorithm was then applied to the outdoor walking data consisting of 15 subjects. Since these signals had poor SNR, all steps were required to detect the gait events. Figure 8 shows the mean and standard deviation of stride time computed for the left and right leg of each subject for outdoor walking.

Table 1: Mean absolute error (MAE) and standard deviation (SD) in seconds for different methods applied on the indoor walking dataset of six subjects.

Method	Gait Event	MAE (SD)
Proposed Method	HS	0.03 (0.01)
	TO	0.01 (0.01)
Symbolic Approach	HS	0.05 (0.04)
	TO	0.03 (0.04)
Peak Detection	HS	0.07 (0.10)
	TO	0.03 (0.03)

5 CONCLUSIONS & DISCUSSION

Most previous methods on gait event detection have been developed for data collected indoors during controlled lab experiments that provide gait events for only a couple of steps. This paper presents a novel algorithm which combines known gait characteristics with wavelet analysis to robustly identify the gait events, HS and TO, from accelerometer signals collected in indoor as well as outdoor walking. The developed method uses resultant accelerometer signal which eliminates the need to know the specific orientation or alignment of the sensor. For indoor walking, the proposed algorithm detects gait events with higher accuracy (Table 1) in comparison to the results of symbolic approach and peak detection method reported in (Sant'Anna and Wickström, 2010). Steps 1 and 4 were sufficient to identify the gait events of all subjects indicating that the data has high SNR.

Analyzing the noisy HSs and TOs in the acceleration signals of the outdoor data (examples shown

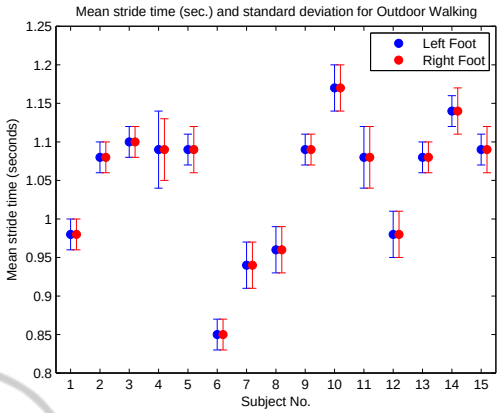

Figure 8: Mean stride time (sec.) and standard deviation for left and right foot of all 15 subjects for outdoor walking.

in Figure 5 and 6) reveals that it has a much lower SNR in comparison to the indoor data. The extra steps needed to detect gait events from outdoor data indicate the uncertainty in applying existing algorithms developed by using indoor data with high SNR. Due to lack of foot switches during outdoor walking experiments, the detected gait events could not be compared to ground truth. However, for a healthy subject walking at their preferred walking speed, the stride time of both feet should be similar with analogous mean stride time as presented in Figure 8; thus substantiating the robustness of the proposed algorithm. This makes it useful for long-term and continuous gait monitoring applications. Using foot switches as ground truth and performing the analysis in real-time are considered for future work.

The use of gait expert knowledge in the algorithm allows a robust analysis. Depending on the quality of the acquired signal and the desired application, it allows the user to decide to either skip or execute steps 2 and 3 (Section 4). This encourages the future possibility to adapt the proposed methodology to other types of data and complex gait. Additionally, each of the four steps of the proposed algorithm provide an insight into the quality of the collected accelerometer signal which can be further analyzed to define a 'data quality index'. This could prove useful to clinicians and researchers to determine the utility of the collected data and run diagnostics accordingly.

REFERENCES

Addison, P. S. (2005). Wavelet transforms and the ECG: A review. *Physiological Measurement*, 26(5):R155–R199.

Aminian, K. et al. (2002). Spatio-temporal parameters of gait measured by an ambulatory system using minia-

ture gyroscopes. *Journal of Biomechanics*, 35(5):689–699.

Aminian, K. et al. (2004). Evaluation of an ambulatory system for gait analysis in hip osteoarthritis and after total hip replacement. *Gait & Posture*, 20(1):102–107.

Aung, M. et al. (2013). Automated detection of instantaneous gait events using time frequency analysis and manifold embedding. *IEEE Transactions on Neural Systems and Rehabilitation Engineering*.

Callisaya, M. L. et al. (2010). Ageing and gait variability a population-based study of older people. *Age and Ageing*, 39(2):191–197.

Desailly, E. et al. (2009). Foot contact event detection using kinematic data in cerebral palsy children and normal adults gait. *Gait & Posture*, 29(1):76 – 80.

Du, P. et al. (2006). Improved peak detection in mass spectrum by incorporating continuous wavelet transform-based pattern matching. *Bioinformatics*, 22(17):2059–2065.

Forsman, P. et al. (2009). Wavelet analysis to detect gait events. In *EMBC*, pages 424–427.

Gouwanda, D. and Senanayake, S. (2009). Application of hybrid multi-resolution wavelet decomposition method in detecting human walking gait events. In *SOCPAR*, pages 580–585.

Hafner, V. and Bachmann, F. (2008). Human-humanoid walking gait recognition. In *Humanoids 2008*, pages 598–602.

Hanlon, M. and Anderson, R. (2009). Real-time gait event detection using wearable sensors. *Gait & Posture*, 30(4):523–527.

Hausdorff, J. M. (2007). Gait dynamics, fractals and falls: Finding meaning in the stride-to-stride fluctuations of human walking. *Human Movement Science*, 26(4):555–589.

Herman, T. et al. (2005). Gait instability and fractal dynamics of older adults with a cautious gait: why do certain older adults walk fearfully? *Gait & Posture*, 21(2):178–185.

Kavanagh, J. J. and Menz, H. B. (2008). Accelerometry: A technique for quantifying movement patterns during walking. *Gait & Posture*, 28(1):1–15.

Khandelwal, S. and Chevallereau, C. (2013). Estimation of the trunk attitude of a humanoid by data fusion of inertial sensors and joint encoders. In *CLAWAR*, pages 822–830.

Lau, H. and Tong, K. (2008). The reliability of using accelerometer and gyroscope for gait event identification on persons with dropped foot. *Gait & Posture*, 27(2):248–257.

Lee, J. and Park, E. (2011). Quasi real-time gait event detection using shank-attached gyroscopes. *Medical & Biological Engineering & Computing*, 49(6):707–712.

Mallat, S. (1999). *A wavelet tour of signal processing*. Academic Press.

Mansfield, A. and Lyons, G. M. (2003). The use of accelerometry to detect heel contact events for use as a sensor in FES assisted walking. *Medical Engineering & Physics*, 25(10):879–885.

McDonough, A. L. et al. (2001). The validity and reliability of the GAITRite system's measurements: A preliminary evaluation. *Archives of Physical Medicine and Rehabilitation*, 82(3):419–425.

Miller, A. (2009). Gait event detection using a multilayer neural network. *Gait & Posture*, 29(4):542–545.

Mills, P. M. et al. (2007). Agreement between footswitch and ground reaction force techniques for identifying gait events: Inter-session repeatability and the effect of walking speed. *Gait & Posture*, 26(2):323–326.

Pappas, I. et al. (2001). A reliable gait phase detection system. *IEEE Transactions on Neural Systems and Rehabilitation Engineering*, 9(2):113–125.

Rafiee, J. et al. (2011). Wavelet basis functions in biomedical signal processing. *Expert Systems with Applications*, 38(5):6190–6201.

Reelick, M. F. et al. (2009). The influence of fear of falling on gait and balance in older people. *Age and Ageing*, 38(4):435–440.

Rueterbories, J. et al. (2010). Methods for gait event detection and analysis in ambulatory systems. *Medical Engineering & Physics*, 32(6):545–552.

Sant'Anna, A. and Wickström, N. (2010). A symbol-based approach to gait analysis from acceleration signals: Identification and detection of gait events and a new measure of gait symmetry. *IEEE Transactions on Information Technology in Biomedicine*, 14(5):1180–1187.

Selles, R. et al. (2005). Automated estimation of initial and terminal contact timing using accelerometers; development and validation in transtibial amputees and controls. *IEEE Transactions on Neural Systems and Rehabilitation Engineering*, 13(1):81–88.

Socie, M. J. et al. (2013). Gait variability and disability in multiple sclerosis. *Gait & Posture*, 38(1):51–55.

Stolze, H. et al. (2004). Falls in frequent neurological diseases. *Journal of Neurology*, 251(1):79–84.

Tan, C. W. and Park, S. (2005). Design of accelerometer-based inertial navigation systems. *IEEE Transactions on Instrumentation and Measurement*, 54(6):2520–2530.

Torrealba, R. et al. (2010). Statistics-based technique for automated detection of gait events from accelerometer signals. *Electronics Letters*, 46(22):1483–1485.

Williamson, R. and Andrews, B. (2000). Gait event detection for FES using accelerometers and supervised machine learning. *IEEE Transactions on Rehabilitation Engineering*, 8(3):312–319.

Woodman, O. J. (2007). An introduction to inertial navigation. Technical report, Univ. of Cambridge.

Yang, C. et al. (2009). Comparison of public peak detection algorithms for MALDI mass spectrometry data analysis. *BMC Bioinformatics*, 10(1):4.